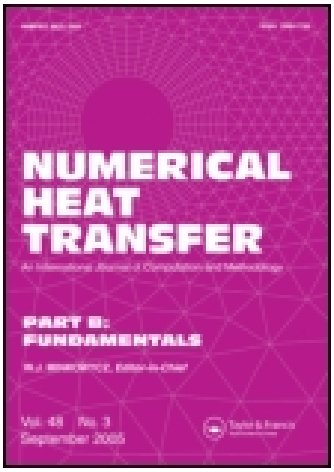

Numerical Heat Transfer, Part B: Fundamentals: An International Journal of Computation and Methodology
Publication details, including instructions for authors and subscription information:
http://www.tandfonline.com/loi/unhb20

On the Limits of Validity of the Low Magnetic Reynolds Number Approximation in MHD Natural-Convection Heat Transfer

I. E. Sarris [a] , G. K. Zikos [a] , A. P. Grecos [a] & N. S. Vlachos [a]
[a] Laboratory of Fluid Mechanics & Turbomachines, Department of Mechanical & Industrial Engineering , University of Thessaly , Volos, Greece
Published online: 24 Feb 2007.

To cite this article: I. E. Sarris , G. K. Zikos , A. P. Grecos & N. S. Vlachos (2006) On the Limits of Validity of the Low Magnetic Reynolds Number Approximation in MHD Natural-Convection Heat Transfer, Numerical Heat Transfer, Part B: Fundamentals: An International Journal of Computation and Methodology, 50:2, 157-180

To link to this article: http://dx.doi.org/10.1080/10407790500459403

Numerical Heat Transfer, Part B, 50: 157–180, 2006

ISSN: 1040-7790 print/1521-0626 online
DOI: 10.1080/10407790500459403

Taylor & Francis
Taylor & Francis Group

ON THE LIMITS OF VALIDITY OF THE LOW MAGNETIC REYNOLDS NUMBER APPROXIMATION IN MHD NATURAL-CONVECTION HEAT TRANSFER

I. E. Sarris, G. K. Zikos, A. P. Grecos, and N. S. Vlachos
Laboratory of Fluid Mechanics & Turbomachines, Department of Mechanical & Industrial Engineering, University of Thessaly, Volos, Greece

In the majority of magnetohydrodynamic (MHD) natural-convection simulations, the Lorentz force due to the magnetic field is suppressed into a damping term resisting the fluid motion. The primary benefit of this hypothesis, commonly called the low-R_m approximation, is a considerable reduction of the number of equations required to be solved. The limitations in predicting the flow and heat transfer characteristics and the related errors of this approximation are the subject of the present study. Results corresponding to numerical solutions of the full MHD equations, as the magnetic Reynolds number decreases to a value of 10^{-3}, are compared with those of the low-R_m approximation. The influence of the most important parameters of MHD natural-convection problems (such as the Grashof, Hartmann, and Prandtl numbers) are discussed according to the magnetic model used. The natural-convection heat transfer in a square enclosure heated laterally, and subject to a transverse uniform magnetic field, is chosen as a case study. The results show clearly an increasing difference between the solutions of the full MHD equations and low-R_m approximation with increasing Hartmann number. This difference decreases for higher Grashof numbers, while for Prandtl numbers reaching lower values like those of liquid metals, the difference increases.

1. INTRODUCTION

Natural-convection heat transfer of electrically conducting fluids in enclosures has been the subject of a great number of theoretical, experimental, and numerical investigations, because of its importance in many technological applications such as, for example, the liquid-metal blankets used in fusion reactors [1] (Ha >200). Another important application is the crystal growth (Bridgman or Czochralski) in

Received 25 February 2005; accepted 28 October 2005.

This work was performed in the framework of the Euratom—Hellenic Republic Association and is supported by the European Union within the Fusion Program. The content of this publication is the sole responsibility of the authors, and it does not necessarily represent the views of the Commission or its services.

Dedicated to the memory of our colleague, teacher and friend the late Demosthenes D. Papailiou, Professor Emeritus of the University of Patras, Greece.

The present address of I. E. Sarris is Université Libre de Bruxelles, Physique Statistique et Plasmas, CP 231 Campus Plaine, 1050 Brussels, Belgium.

Address correspondence to N. S. Vlachos, Laboratory of Fluid Mechanics & Turbomachines, Department of Mechanical & Industrial Engineering, University of Thessaly, Athens Avenue, 38334 Volos, Greece. E-mail: vlachos@mie.uth.gr

NOMENCLATURE

c_p	specific heat	x, y	spatial coordinates
g	gravitational acceleration	X, Y	dimensionless coordinates
Gr	Grashof number	α	thermal diffusivity
H	enclosure height	β	coefficient of thermal expansion
Ha	Hartmann number	Θ	nondimensional temperature
j	current density	$\bar{\mu}$	magnetic permeability
J	dimensionless current density	ν	fluid kinematic viscosity
k	thermal conductivity	ρ	fluid density
Nu	Nusselt number	σ	electrical conductivity
p	fluid pressure	ϕ	generalized variable
P	dimensionless pressure	Ψ	nondimensional streamfunction
Pr	Prandtl number		
R_m	magnetic Reynolds number	**Subscripts**	
t	time	c	centerline
T	fluid temperature	max	maximum
u, v	velocity components in x and y directions	x, y, z	coordinate indices
U, V	dimensionless velocity components	0	reference value

industrial production of semiconductors [2–4] (Ha $<$ 200). Furthermore, numerical studies of magnetohydrodynamics (MHD) natural convection were conducted in order to answer a variety of fundamental questions such as, for example, the effect of the external magnetic field direction on the flow field in cubes [5, 6] or on the heat transfer [7]. Studies of natural-convection flow in rectangular enclosures with transverse magnetic fields have been reported in, among others, [8–11] and with vertical magnetic fields in [12], as well as in porous enclosures [13, 14]. Buoyant MHD flows in ducts have also been studied [15, 16]. Studies of multidimensional or complex configurations, stability, or turbulence have also been carried out for a variety of MHD flows (for example, [17–19]).

The purpose of the mathematical and numerical models used in the majority of the above studies was to determine the influence of any combination of the Grashof, Reynolds, Prandtl, or Hartmann numbers on the flow and heat transfer. A common technique in all these studies was the simplification of the magnetic induction equation through the low-R_m (or quasi-static) approximation [20, 21]. The dimensionless magnetic Reynolds number $R_m(=\bar{\mu}\sigma u_0 L)$ of the flow represents the ratio of advection to diffusion in the magnetic field. At the limit when $R_m \to 0$, magnetic diffusion dominates over convection, and as a consequence the fluid motion has no influence on the magnetic field distribution. Then, the latter can be calculated as if the fluid were at rest and the Lorentz (or Laplace) force of the magnetic field can be evaluated through a damping term, which includes only the velocity, an electric potential, and the external magnetic field. The magnitude of R_m in laboratory-scale experiments (e.g., molten metals) cannot exceed the value of 10^{-2}, and in industrial applications the value of several tenths [20].

Generally accepted in MHD natural-convection numerical studies (for example, [5, 7–10, 12]) is that $R_m \ll 1$, which allows one to overcome the solution of the magnetic induction equations, thus resulting in a significant reduction of the equations to be solved and of computational cost. These studies adopted the

low magnetic Reynolds number approximation (low-R_m model) as a suitable model for the simulation, without any further investigation of the validity of the model for the specific configuration and the range of operational parameters used. Possible differences in the results related to the use of different simulation models can be encountered in the computations of the flow and heat transfer quantities, the most important of which, from the technological point of view, is the Nusselt number. Thus, the knowledge of the possible differences and the parameter space where these are more pronounced helps to increase the confidence of the applications related to MHD heat transfer. The present study is the only one dealing with this issue as concerning the MHD natural convection.

The purpose of the present study, therefore, is to determine the influence of the magnetic Reynolds number, R_m, on the MHD natural-convection flow and heat transfer and to assess possible errors related to the use of the low-R_m approximation. The results of the full magnetic induction equations with the lowest R_m value of 10^{-3} used here are compared throughout this article with those of the low-R_m model. As a case study, the natural-convection heat transfer on a laterally heated square enclosure subjected to a uniform transverse magnetic field was used. In modeling such a system, several factors should be taken into account, in particular, possible inhomogeneities of the (strong) external magnetic field and the three-dimensionality of the enclosure. Numerical simulations of buoyancy-driven flows in cubic enclosures subject to a static homogeneous magnetic field [5–7] have led to some interesting results. However, and despite their limited physical significance, investigations of two-dimensional flows, because of their simplicity, permit one to analyze in more detail the dependence of the flow on parameters of the problem which are varied in a relatively broad range. The limits of the validity of the low-R_m approximation results are studied for a representative range of the important parameters (Gr, Ha, and Pr), and useful conclusions are drawn.

2. MATHEMATICAL ANALYSIS

2.1. Full MHD Equations

The governing equations (mass, momentum, and energy conservation) of natural-convection heat transfer of an incompressible, electrically conducting fluid subjected to an external magnetic field read as follows:

$$\nabla \cdot \mathbf{v} = 0 \tag{1}$$

$$\rho \frac{\partial \mathbf{v}}{\partial t} + \rho(\mathbf{v} \cdot \nabla)\mathbf{v} = -\nabla p + \mu \nabla^2 \mathbf{v} - \rho \mathbf{g} \beta \, \Delta T + \mathbf{j} \times \mathbf{B} \tag{2}$$

$$\frac{\partial T}{\partial t} + (\mathbf{v} \cdot \nabla) T = \frac{k}{\rho c_p} \nabla^2 T \tag{3}$$

where $\mathbf{v}$ is the fluid velocity vector, t the time, p the fluid pressure, ρ the density, μ the molecular viscosity, $\mathbf{g}$ the gravitional acceleration, β the volumetric thermal

expansion coefficient, c_p the fluid specific heat under constant pressure, k its thermal conductivity, and ΔT the difference between the fluid temperature and a characteristic temperature. The term $\rho\mathbf{g}\beta\,\Delta T$ corresponds to the gravitational force due to the existence of temperature gradients according to the Boussinesq approximation, while the cross product $\mathbf{j} \times \mathbf{B}$ between the electric current density $\mathbf{j}$ and the magnetic induction $\mathbf{B}$ denotes the Lorentz (or Laplace) force.

For the present natural-convection flow case, volumetric heat sources such as viscous and ohmic dissipation or nuclear irradiation are assumed to be negligible. As usual in MHD studies, the fluid is assumed to be quasi-neutral and the displacement current is neglected. Thus, Ampére's law, $\bar{\mu}\mathbf{j} = \nabla \times \mathbf{B}$, implies that

$$\mathbf{j} \times \mathbf{B} = \frac{1}{\bar{\mu}}(\nabla \times \mathbf{B}) \times \mathbf{B} = -\frac{1}{2\bar{\mu}}\nabla|\mathbf{B}|^2 + \frac{1}{\bar{\mu}}(\mathbf{B} \cdot \nabla)\mathbf{B} \tag{4}$$

where $\bar{\mu}$ is the magnetic permeability of the medium. Taking into account Faraday's and Ohm's laws, the transport equation for the magnetic induction becomes

$$\frac{\partial \mathbf{B}}{\partial t} + (\mathbf{v} \cdot \nabla)\mathbf{B} - (\mathbf{B} \cdot \nabla)\mathbf{v} = \frac{1}{\bar{\mu}\sigma}\nabla^2\mathbf{B} \tag{5}$$

2.2. The Low-R_m Approximation

The electric current density, $\mathbf{j}$, can be determined from Ohm's law as

$$\mathbf{j} = \sigma(\mathbf{E} + \mathbf{v} \times \mathbf{B}) \tag{6}$$

where the electric field $\mathbf{E}$ and the magnetic field $\mathbf{B}$ satisfy the Maxwell equations, and σ is the electrical conductivity of the fluid.

Assuming negligible perturbations for the electric and magnetic fields, Eq. (6) can be written as

$$\mathbf{j} = \sigma(\mathbf{E_0} + \mathbf{v} \times \mathbf{B_0}) \tag{7}$$

where $\mathbf{E_0}$ and $\mathbf{B_0}$ stand for the respective fields when the fluid is at rest.

Furthermore, because the displacement current is neglected, the electric charge conservation ($\nabla \cdot \mathbf{j} = 0$) implies that $\mathbf{E_0}$ is irrotational and may be replaced by the electric field $(-\nabla V)$, where V is an electrostatic potential.

For a general two-dimensional enclosure without externally supplied electric fields, the divergence of Ohm's law gives

$$\nabla^2 V = \nabla \cdot (\mathbf{v} \times \mathbf{B_0}) = \mathbf{B_0}\left(\frac{\partial \mathbf{v}_x}{\partial y} - \frac{\partial \mathbf{v}_y}{\partial_x}\right) = 0 \tag{8}$$

where $\mathbf{v}_x$ and $\mathbf{v}_y$ are the x- and y-direction fluid velocity components, respectively.

As pointed out by Garandet et al. [11], the harmonic equation for the electric potential ($\Delta^2 \mathrm{V} = 0$) in the case of enclosures with electrically insulating boundaries, on which $\partial_n V = 0$ (n is the normal direction to the boundary) has a unique constant solution $\Delta(\mathbf{V}) = 0$ and thus the electric field vanishes everywhere. The associated

Lorentz force then can be reduced to the damping factor $-|\mathbf{B_0}|^2\mathbf{v}_\perp$, where $\mathbf{v}_\perp$ is the velocity component perpendicular to the direction of $\mathbf{B_0}$.

Considering the above conditions, the Navier-Stokes equation is reduced to

$$\rho\frac{\partial \mathbf{v}}{\partial t} + \rho(\mathbf{v}\cdot\nabla)\mathbf{v} = -\nabla p + \mu\nabla^2\mathbf{v} - \rho\mathbf{g}\beta\,\Delta T - \sigma|\mathbf{B_0}|^2\mathbf{v}_\perp \tag{9}$$

This approximation, called the low-R_m approximation, is commonly used in MHD natural-convection problems. The advantage of using this reduced model instead of the full MHD equations is mainly the reduced number of equations required to be solved (two equations fewer), resulting in lesser computational cost. The errors in the predictions based on this model are discussed below.

2.3. Magnetic Field Perturbation in Natural-Convection Motion

In the low-R_m approximation, all the magnetic perturbations are neglected. The importance of the magnetic Reynolds number (even in laboratory experiments with liquid metals, where it is of order 10^{-3}) was noted by Allen [22]. He proved that a small value of the magnetic Reynolds number does not necessarily mean that diffusion dominates over convection of the magnetic field, and that electromagnetic forces can still play an important role even for small R_m. If $\mathbf{b}$ is the perturbation of the field $\mathbf{B}$ caused by the fluid motion and $\mathrm{B_0}$ is the permanent magnetic field when the fluid is at rest, the total magnetic field is $\mathbf{B} = \mathbf{B_0} + \mathbf{b}$. Allen [22] showed that the ratio of the magnetic convection over diffusion in the modified current equation [$\nabla\times\mathbf{B} = \bar{\mu}\sigma(\mathbf{E} + \mathbf{v}\times\mathbf{B})$, which is the combination of Ampere's and Ohm's laws] is

$$\frac{\text{Convection}}{\text{Diffusion}} = \frac{|\bar{\mu}\sigma(\mathbf{v}\times\mathbf{B})|}{|\nabla\times\mathbf{B}|} \sim R_m\left(\frac{\mathbf{B_0}}{\mathbf{b}}\right)\left(\frac{l_B}{l_v}\right) \tag{10}$$

where l_B and l_v are the length scales for $\mathbf{B}$ and $\mathbf{v}$, respectively. In general, these two length scales may differ, and this is a reason why the convective term of Eq. (5) may be important even at low R_m values.

To estimate the errors due to the low-R_m approximation, the following order-of-magnitude analysis is used. When $R_m \ll 1$, the terms $(\mathbf{v}\cdot\nabla)\mathbf{B}$ and $(\mathbf{B}\cdot\nabla)\mathbf{v}$ [or the equivalent term, $\nabla\times(\mathbf{v}\times\mathbf{B})$] of the induction equation is negligible compared to the diffusion term, indicating that the influence of $\mathbf{v}$ on the field B is very small. The induction equation then becomes

$$\frac{\partial \mathbf{b}}{\partial t} = \nabla\cdot(\mathbf{v}\times\mathbf{B_0}) + \nabla\cdot(\mathbf{v}\times\mathbf{b}) + (\bar{\mu}\sigma)^{-1}\nabla^2\mathbf{b} \tag{11}$$

For steady-state flows and assuming that $|\mathbf{b}| \ll |\mathbf{B_0}|$, the most important terms of this equation are

$$\nabla^2\mathbf{b} + \mu\sigma\nabla\cdot(\mathbf{v}\times\mathbf{B_0}) = 0 \tag{12}$$

It follows that the order of magnitude of the perturbation |b| is $R_m B_0$. Thus, the contribution of the magnetic perturbations increases with increasing magnetic field. This means that the increase of the Hartmann number is expected to influence the agreement of the results between the full MHD equations and the low-R_m approximation.

3. THE TEST CASE

In order to study the influence of the full or low-R_m MHD model on the calculated fields and heat transfer, the common case of the steady-state natural convection in a square enclosure, Figure 1, has been chosen. A temperature difference, ΔT, is imposed at the side walls of the enclosure, while the top and bottom walls are considered adiabatic. Nondimensional quantities are introduced, taking the enclosure's height, H, as the reference length and the quantity ν/H as the reference velocity:

$$\begin{aligned} X &= \frac{x}{H} \qquad Y = \frac{y}{H} \qquad U = \frac{u}{\nu/H} \qquad V = \frac{v}{\nu/H} \\ \Theta &= \frac{T - T_0}{\Delta T} \qquad P = \frac{p' H^2}{\rho \nu} \qquad B = \frac{\mathbf{B}}{B_0} \qquad J = \frac{B_0}{\bar{\mu} H} j \end{aligned} \tag{13}$$

where p' is the total pressure, which includes the so-called magnetic pressure $[(1/2\bar{\mu})B^2]$.

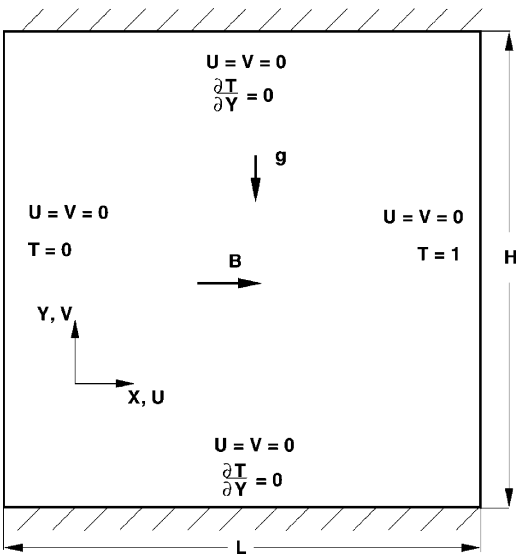

Figure 1. Geometry and boundary conditions of the tests.

Then, the governing equations read as follows:

$$\Delta(\mathbf{V}) = 0 \tag{14}$$

$$(\mathbf{V}\cdot\nabla)\mathbf{V} = -\nabla\mathbf{P} + \nabla^2\mathbf{V} + \mathrm{Gr}\,\Theta + \frac{\mathrm{Ha}^2}{R_m}(\mathbf{B}\cdot\nabla)\mathbf{B} \tag{15}$$

$$(\mathbf{V}\cdot\nabla)\Theta = \frac{1}{\mathrm{Pr}}\nabla^2\Theta \tag{16}$$

$$(\mathbf{V}\cdot\nabla)\mathbf{B} = \frac{1}{R_m}\nabla^2\mathbf{B} + (\mathbf{B}\cdot\nabla)\mathbf{V} \tag{17}$$

$$\mathbf{J} = R_m(\mathbf{V}\times\mathbf{B}) = \nabla\times\mathbf{B} \tag{18}$$

$$\nabla\cdot\mathbf{B} = 0 \tag{19}$$

The dimensionless parameters are the Grashof number, $\mathrm{Gr} = g\beta\,\Delta T\,H^3/\nu^2$, the Prandtl number, $\mathrm{Pr} = \nu/\alpha$, the magnetic Reynolds number, $R_m = \sigma\bar{\mu}\nu$, and the Hartmann number, $\mathrm{Ha}^2 = B_0^2H^2\sigma/\rho\nu$.

In the case of the low-R_m model, the magnetic induction equation is dropped and, using Eq. (9), the momentum equation may be written as

$$(\mathbf{V}\cdot\nabla)\mathbf{V} = -\nabla\mathbf{P} + \nabla^2\mathbf{V} + \mathrm{Gr}\,\Theta - \mathrm{Ha}^2\,|\mathbf{B}|^2\mathbf{V}_\perp \tag{20}$$

with $\mathbf{V}_\perp$, the velocity component perpendicular to the direction of the external field (the V velocity component in the present case).

The boundary conditions are as follows:

$$\begin{array}{llllll}
U = V = 0 & \text{and} & \dfrac{\partial\Theta}{\partial Y} = 0 & \text{for} & Y = 0,1 & 0 \le X \le 1 \\
U = V = 0 & \text{and} & \Theta = 0 & \text{for} & X = 0 & 0 \le Y \le 1 \\
U = V = 0 & \text{and} & \Theta = 1 & \text{for} & X = 1 & 0 \le Y \le 1 \\
B_x = 1 & \text{for} & X = 0,1 & \text{and} & Y = 0,1 & 0 \le Y \le 1 \\
B_y = 0 & \text{for} & X = 0,1 & \text{and} & Y = 0,1 & 0 \le Y \le 1
\end{array} \tag{21}$$

The direction of the magnetic vector, $\mathbf{B}(B_0, 0,0)$, is normal to the gravitational acceleration. The walls are assumed to be electrically insulated, and thus no special wall model is needed (such as, for example, the thin-wall model of [21]). Moreover, the fluid considered is not ferromagnetic and, for simplicity, its relative permeability $\mu_r\,(\approx 1)$ is taken equal to unity. The Hartmann number is varied in the range $0 \le \mathrm{Ha} \le 100$, and the magnetic Reynolds number may take the values 0.001, 0.01, 0.1, and 1.0. The Grashof number is varied in the range from 10^2 to 10^6, while fluids with Prandtl numbers from 0.01 to 7 are considered.

The intensity of the flow circulation inside the enclosure may be measured by the streamfunction value $\Psi(U = \partial\Psi/\partial Y,\ V = -\partial\Psi/\partial X)$. The reference value $\Psi = 0$ of the stream function corresponds to the position $X = 0$ and $Y = 0$. The local Nusselt number Nu_y at the heated or cooled wall is calculated from the temperature field:

$$\mathrm{Nu}_y = -\left|\frac{\partial\Theta}{\partial X}\right|_{X=0 \text{ or } 1} \tag{22}$$

and the average Nusselt number at each side wall is given by

$$\mathrm{Nu} = \int_{Y=0}^{1} \mathrm{Nu}_y \, dY \tag{23}$$

For the present two-dimensional case, the electric current field is calculated from the relationship

$$J_z = \frac{\partial B_y}{\partial x} - \frac{\partial B_x}{\partial y} \tag{24}$$

The differences between the results of the full magnetic induction equation model and the low-R_m model are calculated in terms of the relative error between the values of the two models:

$$E(R_m) = \frac{|\phi(R_m) - \phi(\text{low-}R_m)|}{\phi(R_m)} \times 100\% \tag{25}$$

where ϕ represents the calculated value of maximum streamfunction, Nusselt number, etc.

Thus, the quantity $E(0.001)$ is used throughout this work to give the relative error of a variable, calculated for the same group of nondimensional parameters, between the solution of $R_m = 0.001$ and the low-R_m model.

3.1. Numerical Procedure

The above governing equations together with the corresponding boundary conditions are solved numerically, employing a finite-volume method. The coupling between momentum and continuity equations is achieved using the SIMPLE algorithm [23], with a nonuniform staggered grid in both the horizontal and vertical directions. A finer distribution for the grid nodes close to the walls is used in both directions in order to resolve better the flow and Hartmann boundary layers and to predict efficiently the heat transfer at the conductive walls. The equations for U and V, energy, and magnetic induction are solved using the QUICK scheme of Leonard [24] in the stable form proposed by Hayase et al. [25] in order to minimize numerical diffusion. In all calculations presented here, underrelaxation factors with values of 0.5, 0.5, 0.6, 0.6, 0.6, and 0.3 were applied to U, V, Θ, B_x, B_y, and P, respectively. The iterative procedure is initiated with an arbitrary velocity field

followed by the solution of the energy and magnetic induction equations and is continued until convergence is achieved. Convergence is established when the sum of the absolute relative errors for each solved quantity in the entire flow field is less than a small value ϵ equal to 10^{-5}. All calculations are carried out on Intel CPU-based personal computers.

The present models, in the form of an in-house computational fluid dynamics (CFD) code, have been validated successfully against the works of de Vahl Davis [26] and Janssen and Henkes [27] for steady-state natural-convection heat transfer in enclosures. Extensive description of the performance of the numerical algorithms used here may be found in [28, 29]. The performance of the MHD part of the model was tested against the results of Al-Najem et al. [10], for their low-R_m approximation model of natural convection in a square enclosure, for Grashof numbers 10^4 and 10^6 and for Hartmann numbers in the range 0 to 100.

The comparison between the results of the present models (full and low-R_m) and those in [10] are shown in Table 1 using the nondimensional quantities and grid arrangement of [10]. The maximum horizontal velocity in the midsection and the average Nu are practically the same for every value of Ha for the case of $\mathrm{Gr} = 10^4$. However, the values of Nu in the case of $\mathrm{Gr} = 10^6$ show a small divergence, probably due to differences related to the solution procedures. The present model predicts higher maximum values of the velocities at the enclosure midsection and lower values of Nu in comparison with the results of [10].

In order to show the effect of the choice of magnetic induction model for the present calculations, the results of the full magnetic equations with $R_m = 10^{-3}$ were added in Table 1. The general remark is that the predicted values of velocity and Nusselt number with $R_m = 10^{-3}$ are higher than those using the low-R_m model. As the Hartmann number increases, the relative errors also increase. For the case of $\mathrm{Gr} = 10^6$ and $\mathrm{Ha} = 100$, the maximum relative errors the velocity and Nusselt number between the results of [10] and the present model with $R_m = 10^{-3}$ were 50% and 21%, respectively. In Table 1 of [10] there is a summary of parameters used in several MHD natural-convection cases, where it appears that studies with Ha values of even 1,000 have been conducted using the low-R_m model. An additional proof of the

Table 1. Comparison of present calculations (low-R_m and full magnetic induction model for $R_m = 10^{-3}$) with those of Al-Najem et al. [10]

		$U_{c,\max}$			Nu		
			Present			Present	
Gr	Ha	Ref. [10]	low-R_m	$R_m = 10^{-3}$	Ref. [10]	low-R_m	$R_m = 10^{-3}$
10^4	0	0.19	0.194		2.02	2.06	
	10	0.135	0.138	0.153	1.75	1.738	1.833
	50	0.026	0.025	0.041	1.05	1.022	1.055
10^6	0	0.087	0.084		8.8	9.012	
	10	0.082	0.081	0.083	8.7	8.86	8.915
	25	0.078	0.074	0.082	8.0	7.95	8.404
	100	0.044	0.04	0.064	3.9	3.38	4.732

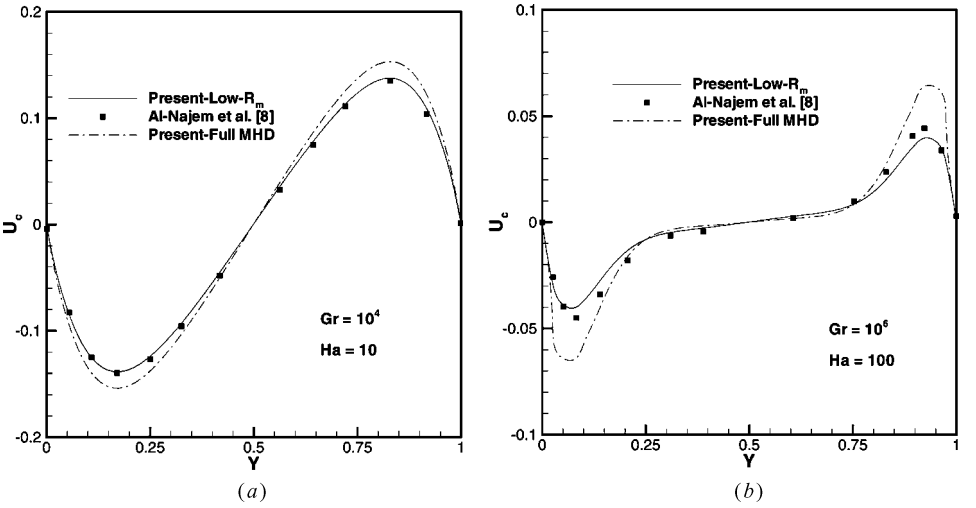

Figure 2. Comparison of the midsection velocity between the present low-R_m and full MHD models for $R_m = 10^{-3}$ and the results of [10]: (*a*) $\mathrm{Gr} = 10^4$, $\mathrm{Ha} = 10$; (*b*) $\mathrm{Gr} = 10^6$, $\mathrm{Ha} = 100$.

different results calculated from each magnetic induction model is given in Figure 2 for two of the cases studied by Al-Najem et al. [10]. For the moderate values of $\mathrm{Gr} = 10^4$ and $\mathrm{Ha} = 10$ shown in Figure 2*a*, in which the present results of the low-R_m model are in good agreement with [10], the full magnetic induction model with $R_m = 10^{-3}$ predicts approximately 18% higher midsection maximum velocity. The difference is higher for the stronger convection case of $\mathrm{Gr} = 10^6$ with $\mathrm{Ha} = 100$ shown in Figure 2*b*.

Before the final calculations, a grid independence test was conducted in order to determine the optimum grid size. The most convective case was selected for this test because of the increasing sensitivity of the nonlinear convective terms to grid refinement. The calculated field values for a grid size of 121×121 for the highly convective case showed that the maximum streamfunction and the average Nusselt number differ by less than 0.01% from the next finer grid (161×161) used, and so this grid was considered adequate for the purposes of the present study. Finally, in all computations presented here, it has been checked that the divergence of the magnetic induction calculated from Eq. (17) vanishes [i.e., Eq. (19) is satisfied within the computer accuracy].

4. RESULTS AND DISCUSSION

4.1. MHD Model Effect on the Flow and Temperature Fields

The results presented below concern cases in which the fluid Prandtl number is 0.7. The influence of Prandtl number on the magnetic induction model used is studied separately in Section 4.3. Streamlines, isotherms, and all other contour plots presented are divided into 15 equally spaced intervals between the lower and the higher values. The range of the values of each plot is given separately in the caption of each

figure. The relative error associated with the calculated quantities is mainly between the full magnetic induction case of $R_m = 0.001$ and the low-R_m model, which correspond to laboratory-scale configurations. This error is generally higher as the R_m increases (i.e., in industrial-scale flows).

The effect of the magnetic Reynolds number on the natural-convection heat transfer inside the square enclosure may be demonstrated by considering the representative flow patterns and the distribution of isotherms in Figures 3 and 4 for

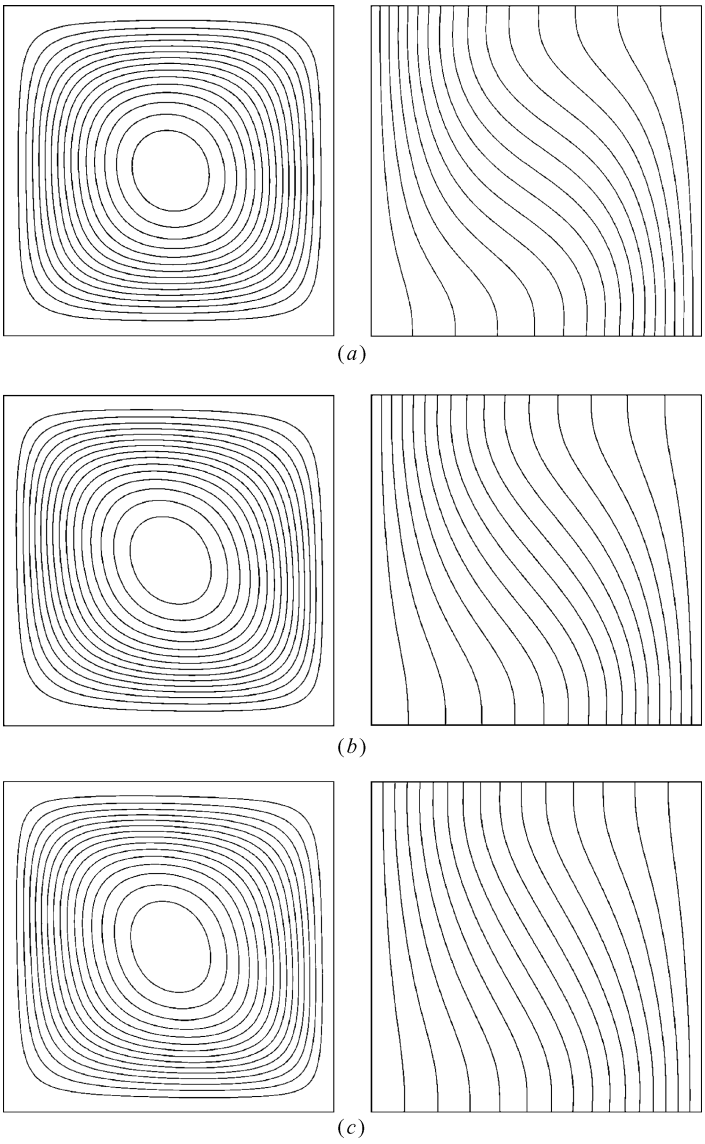

Figure 3. Streamlines (left) and isotherms (right) for $\mathrm{Gr} = 10^4$, $\mathrm{Ha} = 25$: (*a*) $R_m = 1.0$ (0 (0.21) 3.168, 0 (0.065) 1); (*b*) $R_m = 0.001$ (0 (0.149) 2.246, 0 (0.065) 1); (*c*) low-R_m model (0 (0.11) 1.664, 0 (0.065) 1).

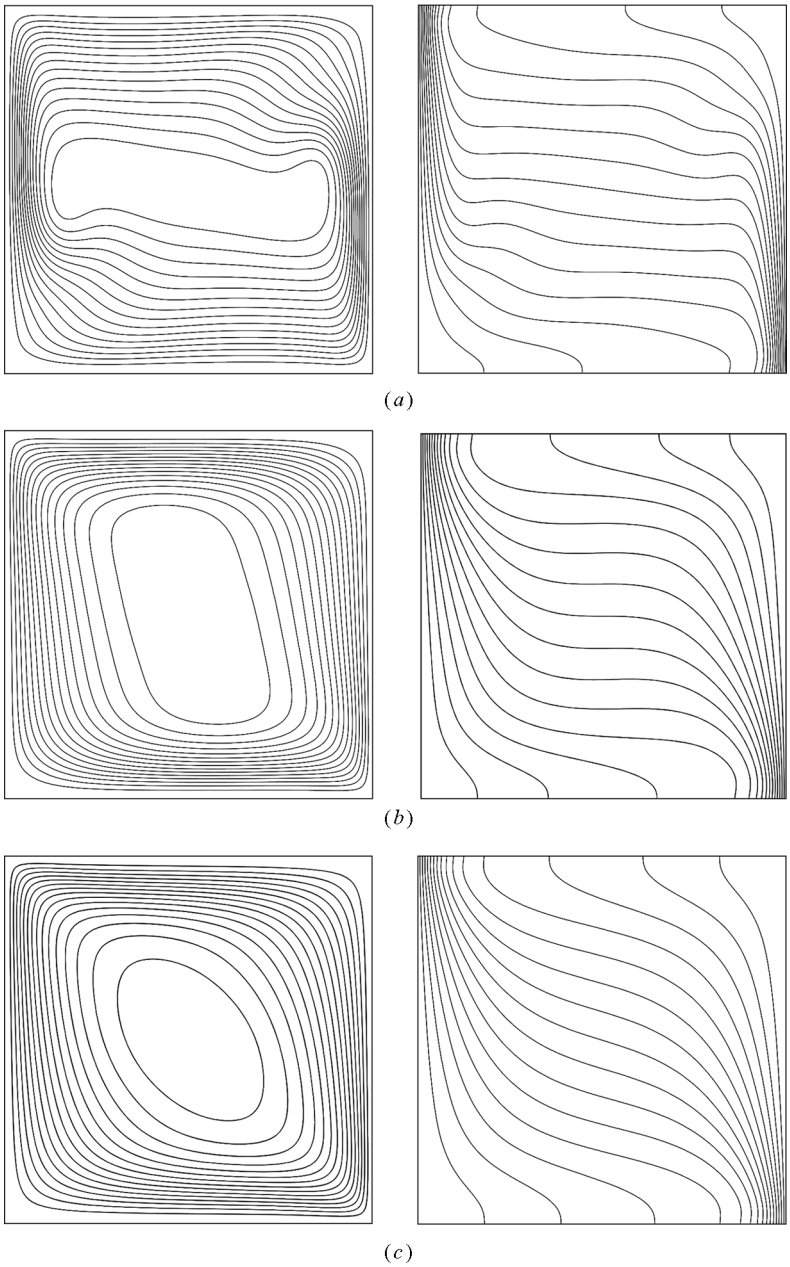

Figure 4. Streamlines (left) and isotherms (right) for $\mathrm{Gr} = 10^6$, $\mathrm{Ha} = 100$: (*a*) $R_m = 1.0$ (−0.018 (1.2) 18.033, 0 (0.065) 1); (*b*) $R_m = 0.001$ (−0.003 (0.61) 9.177, 0 (0.065) 1); (*c*) low-R_m model (0 (0.482) 7.23, 0 (0.065) 1).

two different Grashof and Hartmann numbers. Figure 3 corresponds to the case of $\mathrm{Gr} = 10^4$, $\mathrm{Ha} = 25$ and Figure 4 to that of $\mathrm{Gr} = 10^6$, $\mathrm{Ha} = 100$. Figures 3*a* and 4*a* correspond to $R_m = 1.0$, Figures 3*b* and 4*b* to 0.001, and Figures 3*c* and 4*c* to the

low-R_m model. For the lower-Gr case of Figure 3, the temperature distribution is almost the same for all three cases, and the thick boundary layers are not affected significantly by the R_m value of the full induction model or the low-R_m model used. The small curvature of the isotherms indicates that the conduction is the dominant heat transfer mechanism. The streamline patterns for $R_m = 1.0$, in the core region, differ slightly from the other two cases (Figures 3*b* and 3*c*). In spite of the illustrated similarity of the last two streamline patterns, the flow circulation intensity, which is characterized by the maximum value of the streamfunction, $\Psi_{\max}$, is totally different. The decrease of R_m causes a simultaneous decrease of the calculated flow circulation intensity due to the fact that the Lorentz force is inversely proportional [Eq. (15)] to the R_m value. Moreover, the Lorentz force in the low-R_m model has a stronger damping effect on the fluid motion and further underpredicts the velocity field.

The flow patterns and temperature distribution for the case of $\mathrm{Gr} = 10^6$ and $\mathrm{Ha} = 100$ are shown in Figure 4. The combination of these relatively high values of Gr and Ha numbers has a complex effect on the heat transfer mechanism. On one hand, the higher Grashof number enforces the domination of convection over conduction in the fluid flow, and on the other hand, the higher value of the Hartmann number (i.e., increase of the external magnetic field $\mathbf{B_0}$) intensifies the resistance to the fluid motion, resulting in an enhancement of conduction heat transfer. The higher value of Ha selected corresponds to a lower accuracy of the low-R_m model because the error between the full magnetic induction model and the low-R_m model is proportional to Ha^2. This is because for higher values of Ha, the stronger convection flow currents induce higher values of magnetic field and, consequently, the low-R_m approximation produces worse results.

The flow structure of the full induction model, for all the cases of R_m values studied, is completely different from the low-R_m approximation. The resulting streamfunction distribution with decreasing R_m (Figures 4*a* and 4*b*) appear to be totally different. The circulation cell formed for $R_m = 1.0$ is centrally placed and its extent reaches the side walls, forming thinner boundary layers than those for $R_m = 0.001$. Comparing the streamfunction distribution of the full magnetic induction case of $R_m = 0.001$ and the low-R_m model, it appears that they are in better agreement (with some differences only in the core region), forming thick boundary layers. As in the case of lower Gr in Figure 3, the value of $\Psi_{\max}$ depends on the R_m value when the full magnetic induction model is used and is lower for the case of the low-R_m model. The temperature distribution is not affected significantly by R_m (except that the thermal boundary layer becomes thicker with decreasing R_m) or by the low-R_m model. This proves the initial hypothesis that the increase of the Lorentz force (due to decreasing R_m) enhances conduction and reduces the heat transfer through the boundaries.

As a measure of the effect of the R_m on the fluid circulation intensity, the distribution of the maximum value of the streamfunction, $\Psi_{\max}$, is plotted versus Gr and Ha in Figures 5*a* and 5*b*, respectively. The dependence of $\Psi_{\max}$ on Grashof number is demonstrated in Figure 5*a* for the moderate value of $\mathrm{Ha} = 25$ and for $R_m = 1.0$, $R_m = 0.001$, and the low-R_m model. The dependence of $\Psi_{\max}$ on Hartmann number for $\mathrm{Gr} = 10^6$ is shown in Figure 5*b* for the same three cases of R_m. The associated relative error distribution, $E(0.001)$, between the results of the $\Psi_{\max}$ calculated from the full magnetic induction model for $R_m = 0.001$ and those

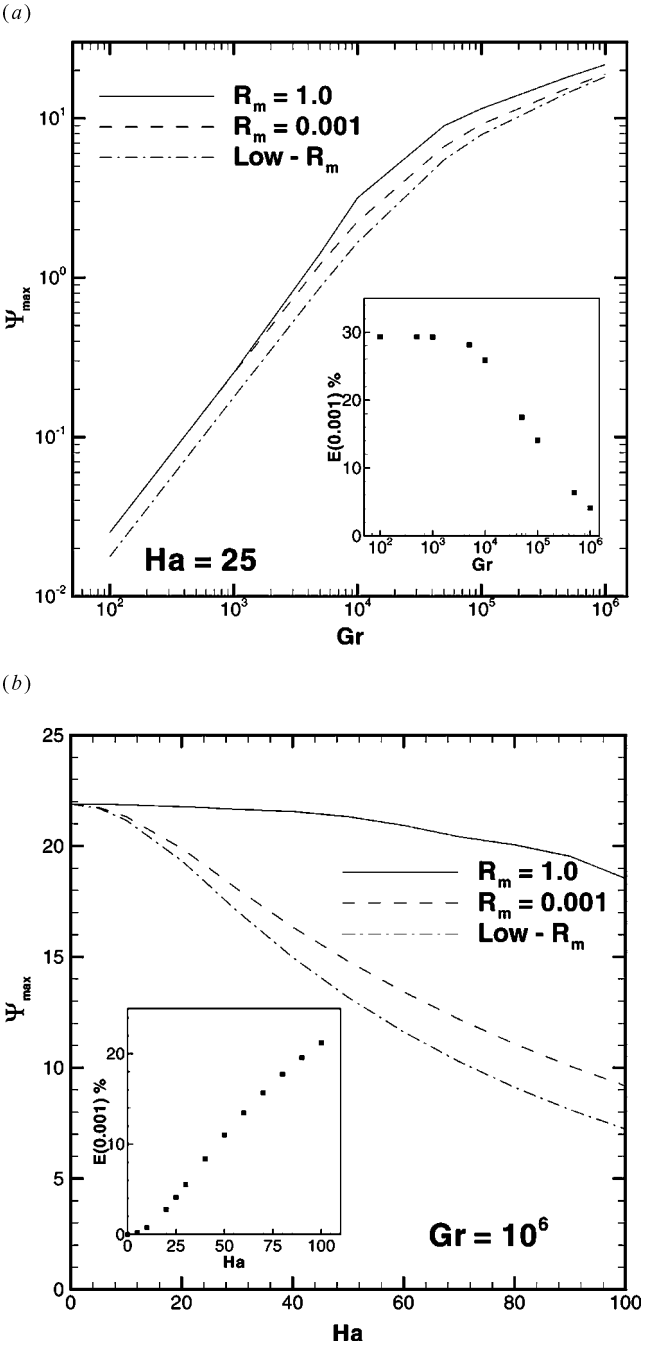

Figure 5. Variation of the maximum value of the streamfunction for $R_m = 1.0$ and 0.001 and the low-R_m model with: (*a*) Grashof number for Ha = 25; (*b*) Hartmann number for Gr = 10^6.

of the low-R_m model are plotted in the inner plots for each case. Connected with the above results, the $\Psi_{\max}$ value is high for the case of $R_m = 1.0$, becoming lower as R_m decreases. The calculated values of $\Psi_{\max}$ for the low-R_m model are lower than those of the full magnetic induction model for all the Gr values studied. For the case of $R_m = 0.001$, the calculated distribution is somewhere between the previous two ($R_m = 1.0$ and low-R_m). For low Gr(=10^2), the flow circulation intensity for the above case is closer to that of $R_m = 1.0$. This is in agreement with the fact that the weak conductive flow (small fluid velocities for low Gr) induces negligible amount of magnetic field due to magnetic diffusion only. The semiconvective term of Eq. (12) $[\nabla \cdot (\mathbf{v} \times \mathbf{B_0})]$ is almost negligible, and the magnetic fluctuations follow only the diffusion law. Thus, the resulting Lorentz force for these cases is independent of the value of R_m. Furthermore, the equivalent Lorentz force of the low-R_m model, which takes into account all the terms of Eq. (12), results in stronger damping than it should.

Alternatively, as Gr increases and the flow is fully convective ($\mathrm{Gr} = 10^6$), the values of $\Psi_{\max}$ from the full magnetic induction model with $R_m = 0.001$ approach those of the low-R_m model. In the convective regime, the intense circulation currents induce a larger amount of magnetic perturbations, $\mathbf{b}$, in the case of $R_m = 1.0$ and significantly less in the case of $R_m = 0.001$, thus matching the requirements of the low-R_m model. The tendency for uniformity of the magnetic field and the formation of thin layers (where the current is concentrated) as the R_m increases is the reason the flow circulation intensity is higher for $R_m = 1.0$ than for $R_m = 0.001$ or for the low-R_m model (proof of this behavior is given in the comments on Figure 6, below). A careful inspection of the relative error between the values of the $\Psi_{\max}$ of the full magnetic induction cases for $R_m = 0.001$ and those of the low-R_m model reveal their reciprocal dependence on Gr. For cases of small Gr, the relative error between the two cases is about 30%, while the increase of Gr reduces this error to less than 5% (for $\mathrm{Gr} = 10^6$).

This latter case of $\mathrm{Gr} = 10^6$, which corresponds to the lowest relative error level, is selected to demonstrate the dependence of $\Psi_{\max}$ on Ha due to the magnetic model used. The distribution of $\Psi_{\max}$ values for the cases of the full magnetic induction model with $R_m = 1.0$ and $R_m = 0.001$ and those of the low-R_m model are shown in Figure 5*b*. As Ha increases, the stronger Lorentz force on the fluid causes its deceleration. The decrease of the circulation intensity depends on both increasing Ha and decreasing R_m. The differences between the results of the full magnetic induction model for $R_m = 0.001$ and the low-R_m model increase monotonically as Ha increases. The relative error curve shows that, for the case of $\mathrm{Ha} = 100$, the associated error exceeds 22%. Considering that in many technological applications (including fusion reactor blankets) the value of the Hartmann number can rise to several thousands, the need to verify the numerical results is more intense.

The effect of R_m on the induced magnetic perturbations and consequently on the electric current patterns and the resulting Lorentz force is shown in Figure 6. The cases considered here correspond to $R_m = 1.0$ in Figure 6*a* and $R_m = 0.001$ in Figure 6*b*, for $\mathrm{Gr} = 10^6$ and $\mathrm{Ha} = 25$. For the higher-R_m case, the induced magnetic perturbations are more than two orders of magnitude higher than for $R_m = 0.001$. For $R_m = 1.0$, regions with high magnetic perturbations are concentrated mainly in the upper-right and bottom-left corners of the enclosure, forming thin boundary

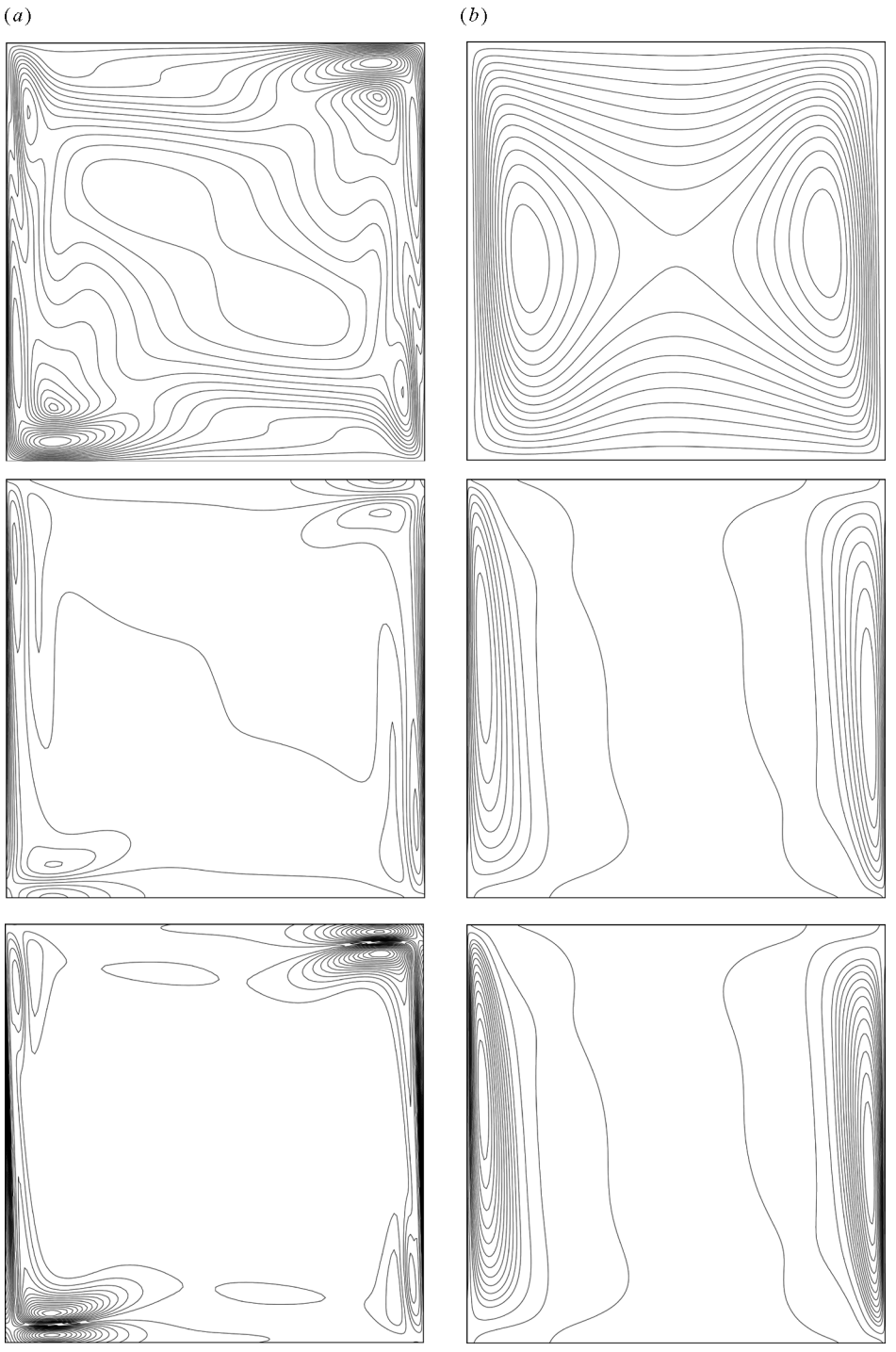

Figure 6. Distribution of magnitude of the magnetic perturbations (upper), electric current (middle), and Lorentz force (lower) for $Gr = 10^6$ and $Ha = 25$: (*a*) $R_m = 1.0$ (0 (0.148) 2.375, –140.26 (17.53) 140.26, 0 (9.87) 148.07); (*b*) $R_m = 0.001$ (0 (0.0008) 0.0128, −0.176 (0.023) 0.176, 0 (11.76) 176.441).

layers. In contrast, for the lower-R_m case, the induced magnetic perturbations are distributed in the vicinity of the side walls. The value of R_m is thus responsible for the displacement of the magnetic perturbations from the side walls to the corners and the horizontal boundaries. The electrical current patterns follow closely the magnetic perturbations and, for the case of $R_m = 0.001$, these patterns cover the entire height of the side walls, forming relatively thick layers, while for the case of $R_m = 1.0$, the higher amount of current passes through thin side wall layers and the upper-right and bottom-left corners.

The resulting Lorentz force distribution also follows the magnetic perturbation and the current patterns. This means that, for the lower-R_m case, the resistance to fluid motion is stronger, concentrated at the side walls, and results in lower circulation intensity and heat transfer than for the case of $R_m = 1.0$. For the present study, in which the horizontal boundaries are both adiabatic, the existence of stronger Lorentz forces in the corners and the horizontal boundaries (for $R_m = 1.0$) does not affect the heat transfer significantly.

4.2. Effect of MHD Model on the Heat Transfer

The magnetic induction model used (full or low-R_m) and the value of R_m also have a significant effect on the heat transfer rates at the side walls, as shown in Figure 7, where the variation of average Nusselt number with Gr and Ha is presented. The average Nusselt number is not affected significantly by the magnetic induction model at low Gr values (Figure 7*a*). For the conduction-dominated flow of $\mathrm{Gr} = 10^2$–10^3, the value of the Nusselt number (equal to 1 for pure conduction) is identical for all the cases of R_m (10 and 0.001) and the low-R_m model. Further increase of Gr increases the values of Nu and, consequently, the associated errors. Upon increasing the value of Gr to 5×10^4, the relative error increases to almost 12%. For the case of $R_m = 1.0$, the values of average Nu are higher than for $R_m = 0.001$ because of the stronger flow currents, while for $R_m = 0.001$ they are closer to those of the low-R_m model. For higher Gr, the relative error decreases and the results of the full magnetic induction model with $R_m = 0.001$ approach those of the low-R_m model.

A stronger effect of the magnetic induction model on Nu values can be observed with increasing Ha, shown in Figure 7*b*, for the higher-convective case of $\mathrm{Gr} = 10^6$ studied. As already discussed, the case of $\mathrm{Gr} = 10^6$ produces smaller relative errors between the results of the full magnetic induction model with $R_m = 0.001$ and the low-R_m model. The distribution of Nu values depends strongly on R_m. The increase of Ha decreases the values of Nu, as expected, through the increase of the magnetic damping action. The relative error between the results of the full magnetic induction model with $R_m = 0.001$ and the low-R_m model increases monotonically as Ha increases (for $\mathrm{Ha} = 100$, the error exceeds 18%). Considering the much higher values of Ha corresponding to the fusion blankets, the error in the estimation of Nu through the choice of magnetic induction model could increase dramatically.

Interesting conclusions on the effect of R_m on the heat transfer and on the validity of the low-R_m approximation may be drawn also from the distribution of the local Nusselt number on the side walls. Figure 8*a* shows the distribution of Nu_y

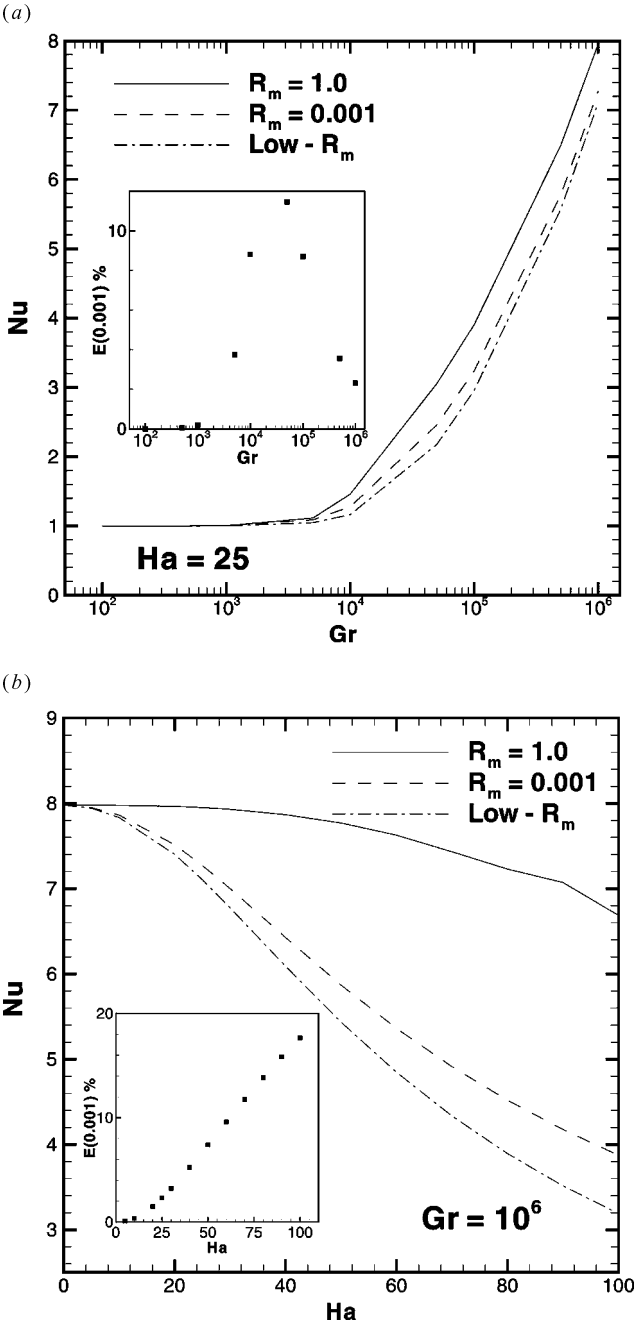

Figure 7. Variation of the average Nusselt number at the hot wall for $R_m = 1.0$ and 0.001 and the low-R_m model with: (*a*) Grashof number for Ha = 25; (*b*) Hartmann number for Gr = 10^6.

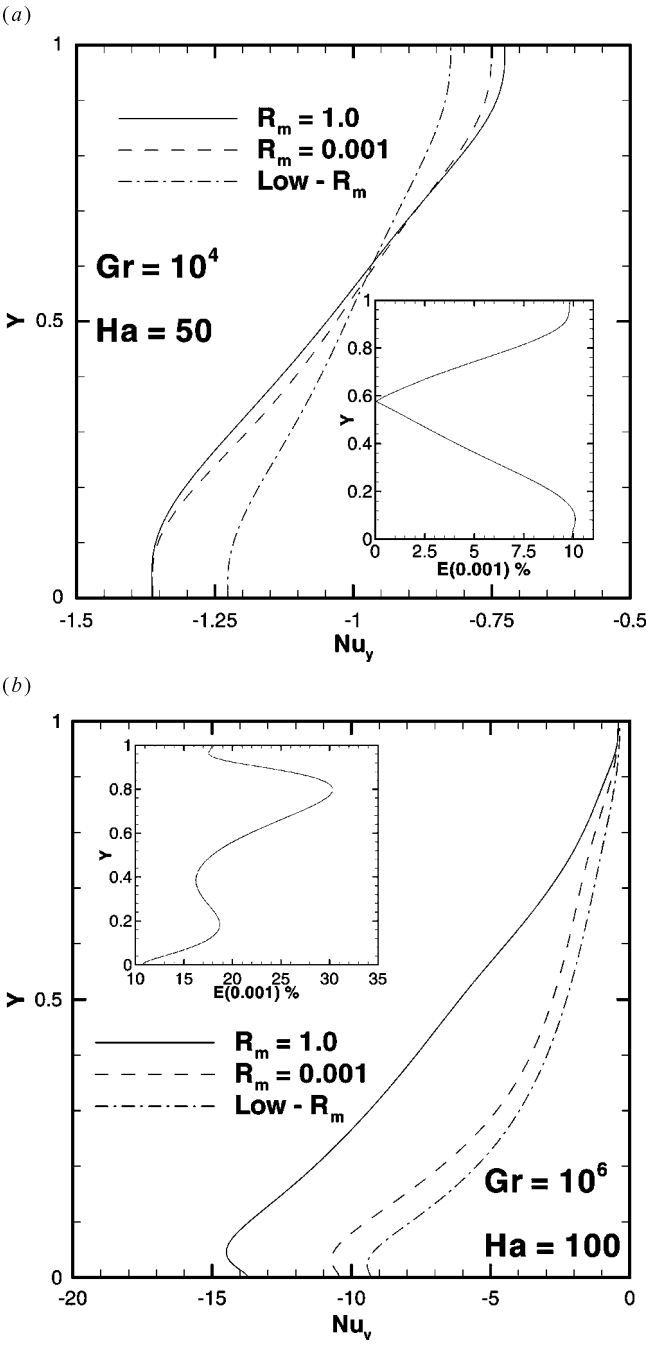

Figure 8. Variation of the local Nusselt number along the cold wall for $R_m = 1.0$ and 0.001 and the low-R_m model for: (*a*) $\mathrm{Gr} = 10^4$ and $\mathrm{Ha} = 50$; (*b*) $\mathrm{Gr} = 10^6$ and $\mathrm{Ha} = 100$.

for the moderate value of $Gr = 10^4$ and for the relatively high value of $Ha = 50$, while Figure 8*b* shows the same distribution for the higher-convective case of $Gr = 10^6$ and the highest value of $Ha = 100$ studied. In the first case, the distributions of the local Nusselt number for $R_m = 1.0$ and $R_m = 0.001$ are very close, and far from the values of the low-R_m model. The stronger flow predicted by the full magnetic induction model corresponds to a higher heat transfer rate than that of the low-R_m model. In the corners of the enclosure, the maximum relative error between the magnetic induction models is approximately 10%. The heat transfer rate distributions for the two different R_m numbers are almost identical because of the slow motion, which cannot give rise to significant perturbations of the magnetic field.

The distributions of the local Nusselt number for the second stronger convective case (Figure 8*b*) follows better the general trend in which the values of $R_m = 0.001$ are closer to those of the low-R_m approximation. In the bottom corner of the hot wall the heat transfer rate is very high, while in the region of the upper corner the heat transfer rate becomes almost zero. The maximum relative error between the results of the full magnetic induction calculation with $R_m = 0.001$ and those of the low-R_m model exceeds locally the value of 30%.

4.3. Prandtl Number Dependence

Electrically conducting fluids with Prandtl numbers in the range between 10^{-2} and 7 were studied next. These values are representative of liquid metals (~ 0.0321), molten mixed-oxide nuclear fuels [~ 0.7 for $(U_{0.8}Pu_{0.2})O_2$], and water–salt solutions (~ 7). The influence of Pr on the fluid circulation intensity and heat transfer are discussed for the full magnetic induction model and the low-R_m model. The case of $Ha = 25$ and $Gr = 10^6$ was selected because it is fairly convective and incorporates low relative errors for $Pr = 0.7$. Figure 9*a* shows the variation of the maximum streamfunction value versus Pr for the cases of $R_m = 1.0$, $R_m = 0.001$, and the low-R_m model. A relative error diagram between the calculated values for $R_m = 0.001$ and the low-R_m model is also included. When Pr is decreased, the relative error increases up to 22% for $Pr = 0.01$. For Pr values higher than 2, the relative error is fixed at a value lower than 2%. These results satisfy the order-of-magnitude analysis, which shows a Pr^{-1} dependence on the associated error through the low-R_m model. The same effect is observed for the variation of Nu versus Pr for the case of $Ha = 25$ and $Gr = 10^6$ shown in Figure 9*b*. The relative error reaches almost 10% for the lower Pr of 0.01 studied, then decreases as Pr increases, and remains practically unchanged (lower than 1%) for Pr values higher than 2.

From the above results it appears that the higher differences for the circulation intensity and the heat transfer between the two magnetic induction models (full or low-R_m) correspond to the lower values of Pr. This means that liquid metal calculations (such as those for liquid metals in many MHD natural-convection applications) with the low-R_m model result in higher relative errors than using the full magnetic induction equations. On the other hand, calculations with working fluids of higher Pr are less sensitive to the magnetic model used. A useful correlation of the Nusselt number as function of Ha, Gr, and Pr can be found in the experimental work of Papailiou and Lykoudis [30].

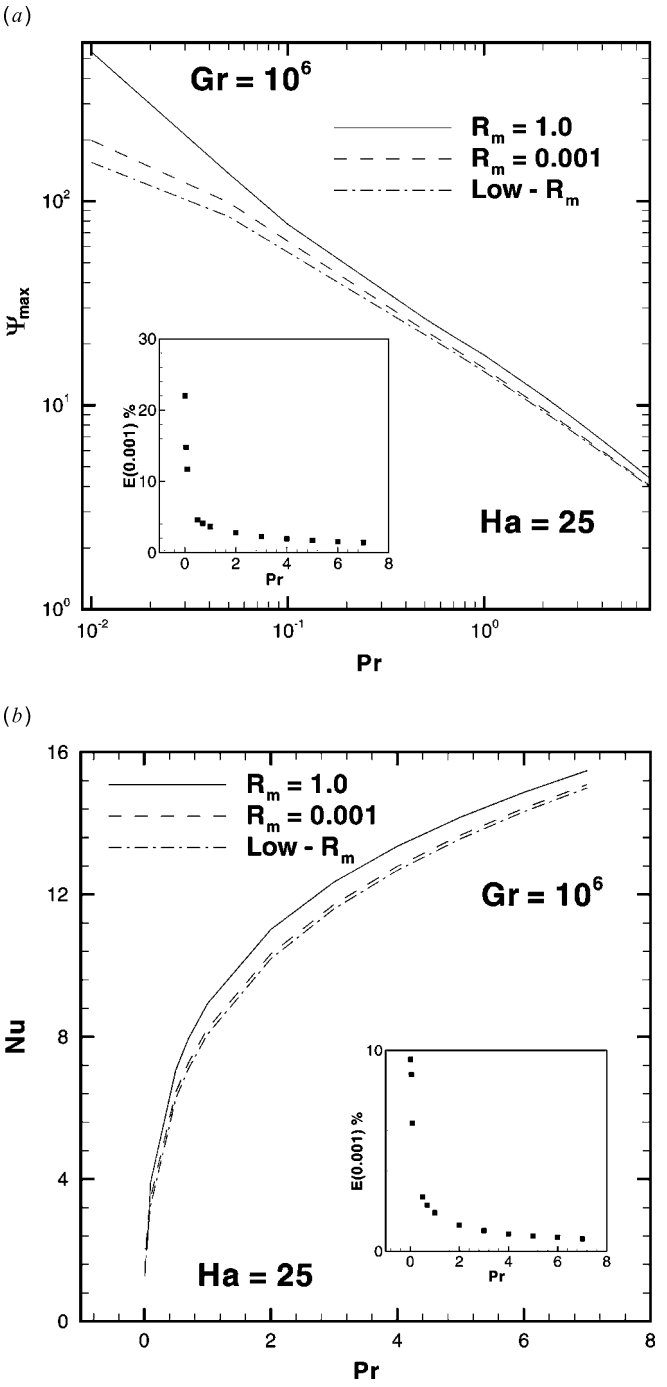

Figure 9. Variation with the Prandtl number of (*a*) the maximum value of the streamfunction and (*b*) the Nusselt number for $R_m = 1.0$ and 0.001 and the low-R_m model for Ha = 25 and Gr = 10^6.

5. CONCLUSIONS

The limits of validity of the low-R_m (or quasi-static) approximation for the case of MHD natural-convection heat transfer were investigated and the dependence of the flow parameters with the associated errors was determined. The case study of a laterally heated square enclosure placed on a uniform magnetic field was used to assess the reliability of the scale analysis and of the magnetic induction model used.

A general observation for the magnetic Reynolds number is that the decrease of its value, for any Grashof and Hartmann numbers, causes a decrease in the flow intensity and heat transfer from the vertical solid boundaries, due to the narrow Hartmann layers which are formed. Moreover, the shapes of the streamlines and isotherms were found to be different between solutions of the low-R_m model and those of the full MHD equations, especially at higher Grashof and Hartmann numbers.

The errors associated with the magnetic induction model used (full equations or low-R_m approximation) in natural-convection heat transfer simulations were calculated. Results show that as the Gr number increases, the differences between the two models become smaller ($<5\%$ of $\Psi_{\max}$ for $\mathrm{Gr} = 10^6$), while as the Ha number increases, the differences become larger ($>20\%$ of $\Psi_{\max}$ and $>18\%$ of Nu for $\mathrm{Ha} = 100$). A mixed behavior of the Nusselt number was observed as Gr is increased (the larger difference was found for $\mathrm{Gr} = 5 \times 10^4$).

A careful comparison of the results of the full magnetic induction model at low R_m values ($=0.001$) with those of the low-R_m approximation shows that, for relatively large Hartmann numbers, the differences in the estimated flow intensity and heat transfer are very large and should be taken into consideration in practical problems. Considering that in many technological applications (including fusion reactor blankets), the value of Ha reaches some thousands, careful choice of the magnetic induction model is essential for the reliability of the results.

The latter conclusion is also true for the effect of Prandtl number on the associated differences between the two magnetic induction models. Results show that when Pr is increased, the difference remains practically small and constant, while for very low values of Pr (such as those of liquid metals), the difference increases significantly. Thus, knowledge of the differences and the parameter space in which they are more pronounced (especially for the case of liquid metals and the presence of strong magnetic fields—a typical situation for crystal growth procedures and fusion blankets) is essential to increase the confidence of applications related to MHD heat transfer. Finally, the present results can help in the correct determination of important heat transfer parameters such as the Nusselt number.

REFERENCES

1. N. B. Morley, S. Smolentsev, L. Barleon, I. R. Kirillov, and M. Takahashi, Liquid Magnetohydrodynamics—Recent Progress and Future Direction for Fusion, *Fusion Eng. Design*, vol. 5l–52, pp. 701–713, 2000.
2. A. Juel, T. Mullin, H. Ben Hadid, and D. Henry, Magnetohydrodynamic Convection in Molten Gallium, *J. Fluid Mech.*, vol. 378, pp. 97–118, 1999.
3. T. Alboussiére, J. P. Garandet, and R. Moreau, Buoyancy-Driven Convection with a Uniform Magnetic Field. Part 1. Asymptotic Analysis, *J. Fluid Mech.*, vol. 253, pp. 545–563, 1993.

4. L. Davoust, M. D. Cowley, R. Moreau, and R. Bolcato, Buoyancy-Driven Convection with a Uniform Magnetic Field. Part 2. Experimental Investigation, *J. Fluid Mech.*, vol. 400, pp. 59–90, 1999.
5. H. Ozoe and K. Okada, The Effect of the Direction of the External Magnetic Field on the Three-Dimensional Natural Convection in a Cubical Enclosure, *Int. J. Heat Mass Transfer*, vol. 32, pp. 1939–l954, 1989.
6. R. Shigemitsu, T. Tagawa, and H. Ozoe, Numerical Computation for Natural Convection of Air in a Cubic Enclosure under Combination of Magnetizing and Gravitational Forces, *Numer. Heat Transfer A*, vol. 43, pp. 449–463, 2003.
7. T. Tagawa and H. Ozoe, Enhancement of Heat Transfer Rate by Application of a Static Magnetic Field during Natural Convection of Liquid Metal in a Cube, *ASME J. Heat Transfer*, vol. 119, pp. 265–271, 1997.
8. S. Alchaar, P. Vasseur, and E. Bilgen, Natural Convection Heat Transfer in a Rectangular Enclosure with a Transverse Magnetic Field, *ASME J. Heat Transfer*, vol. 117, pp. 668–673, 1995.
9. I. E. Sarris, S. C. Kakaratzas, A. P. Grecos, and N. S. Vlachos, MHD Natural Convection in a Laterally and Volumetrically Heated Square Cavity, *Int. J. Heat Mass Transfer*, vol. 48, pp. 3443–3453, 2005.
10. N. M. Al-Najem, K. M. Khanafer, and M. M. El-Rafaee, Numerical Study of Laminar Natural Convection in Tilted Enclosure with Transverse Magnetic Field, *Int. J. Numer. Meth. Heat Fluid Flow*, vol. 8, pp. 651–672, 1998.
11. J. P. Garandet, T. Alboussiere, and R. Moreau, Bouyancy Driven Convection in a Rectangular Enclosure with a Transverse Magnetic Field, *Int. J. Heat Mass Transfer*, vol. 35, pp. 741–748, 1992.
12. N. Rudraiah, R. M. Barron, M. Venkatachalappa, and C. K. Subbaraya, Effect of a Magnetic Field on Free Convection in a Rectangular Enclosure, *Int. J. Eng. Sci.*, vol. 33, pp. 1075–1084, 1995.
13. K. M. Khanafer and A. J. Chamkha, Hydromagnetic Natural Convection from an Inclined Porous Square Enclosure with Heat Generation, *Numer. Heat Transfer A*, vol. 33, pp. 891–910, 1998.
14. S. Alchaar, P. Vasseur, and E. Bilgen, Hydromagnetic Natural Convection in a Tilted Rectangular Porous Enclosure, *Numer. Heat Transfer A*, vol. 27, pp. 107–127, 1995.
15. L. Bühler, Laminar Buoyant Magnetohydrodynamic Flow in Vertical Rectangular Ducts, *Phys. Fluids*, vol. 10, pp. 223–236, 1998.
16. U. Müller and L. Bühler, *Magnetofluiddynamics in Channels and Containers*, Springer-Verlag, Berlin, 2001.
17. S. Kaddeche, D. Henry, and H. Benhadid, Magnetic Stabilization of the Buoyant Convection between Infinite Horizontal Walls with a Horizontal Temperature Gradient, *J. Fluid Mech.*, vol. 480, pp. 185–216, 2003.
18. D. S. Krasnov, E. Zienicke, O. Zikanov, T. Boeck, and A. Thess, Numerical Study of the Instability of the Hartmann Layer, *J. Fluid Mech.*, vol. 504, pp. 183–211, 2004.
19. D. Lee and H. Choi, Magnetohydrodynamic Turbulent Flow in a Channel at Low Magnetic Reynolds Number, *J. Fluid Mech.*, vol. 439, pp. 367–394, 2001.
20. R. Moreau, *Magnetohydrodynamics*, Kluwer, London, 1990.
21. P. A. Davidson, *An introduction to Magnetohydrodynamics*, Cambridge University Press, Cambridge, UK, 2001.
22. J. E. Allen, A Note on the Magnetic Reynolds Number, *J. Phys. D: Appl. Phys.*, vol. 19, pp. L133–Ll35, 1986.
23. S. V. Patankar and D. B. Spalding, A Calculation Procedure for Heat, Mass and Momentum Transfer in Three-Dimensional Parabolic Flows, *Int. J. Heat Mass Transfer*, vol. 15, pp. 1787–1806, 1972.

24. B. P. Leonard, A Stable and Accurate Convective Modelling Procedure Based on Quadratic Upstream Interpolation, *Comput. Meth. Appl. Mech. Eng.*, vol. 19, pp. 59–98, 1979.
25. T. Hayase, J. A. C. Humphrey, and R. Greif, A Consistently Formulated QUICK Scheme for Fast and Stable Convergence Using Finite-Volume Iterative Calculation Procedure, *J. Comput. Phys.*, vol. 98, pp. 108–118, 1992.
26. G. De Vahl Davis, Natural Convection of Air in a Square Cavity: A Bench Mark Numerical Solution, *Int. J. Numer. Meth. Fluids*, vol. 3, pp. 249–264, 1983.
27. R. J. A. Janssen and R. W. M. Henkes, Accuracy of the Finite-Volume Discretizations for the Bifurcating Natural Convection Flow in a Square Cavity, *Numer. Heat Transfer*, vol. 24, pp. 192–207, 1993.
28. I. E. Sarris, I. Lekakis, and N. S. Vlachos, Natural Convection in a 2D Enclosure with Sinusoidal Upper Wall Temperature, *Numer. Heat Transfer A*, vol. 42, pp. 513–530, 2002.
29. I. E. Sarris, I. Lekakis, and N. S. Vlachos, Natural Convection in Rectangular Tanks Heated Locally from Below, *Int. J. Heat Mass Transfer*, vol. 47, pp. 3185–3216, 2004.
30. D. D. Papailiou and P. S. Lykoudis, Magneto-Fluid-Mechanics Free Convection Turbulent Flow, *Int. J. Heat Mass Transfer*, vol. 17, pp. 1181–1189, 1974.